

## Short Communication

# Natural history of experimental arthritis induced by *Paracoccidioides brasiliensis* in wistar rats

Eduardo Alexandre Loth<sup>[1]</sup>, Vanessa Cecatto<sup>[1]</sup>, Rodrigo Daniel Genske<sup>[2]</sup>,  
Maricília Silva Costa<sup>[2]</sup>, Rinaldo Ferreira Gandra<sup>[1]</sup>  
and Cleverson Marcelo Pilatti<sup>[2]</sup>

[1]. Laboratório Experimental de Microbiologia e Análises Clínicas, Ensino, Pesquisa e Extensão,  
Universidade Estadual do Oeste do Paraná, Cascavel, PR, Brasil.

[2]. Instituto de Pesquisa e Desenvolvimento, Universidade do Vale do Paraíba, São José dos Campos, SP, Brasil.

### Abstract

**Introduction:** Paracoccidioidomycosis (PCM) is the most prevalent systemic mycosis in Latin America. This study aimed to evaluate the natural history of *Paracoccidioides brasiliensis*-induced experimental arthritis of the knee joints in Wistar rats. **Methods:** Rats were randomly allocated to either an absolute control group, or 15-day, 45-day, or 90-day experimental (fungus-inoculated) groups. **Results:** Experimental groups developed classic signs of articular PCM. Titers of anti-gp43 were observed to increase during the interval from 15 to 45 days post-inoculation. **Conclusions:** Articular arthritic lesions were induced and progressed during the study period in all experimental groups.

**Keywords:** Arthritis. Paracoccidioidomycosis. *Paracoccidioides brasiliensis*.

Paracoccidioidomycosis (PCM) is a systemic mycosis caused by the fungus *Paracoccidioides brasiliensis* (Pb), initially known as Brazilian blastomycosis, South American blastomycosis, or Lutz-Almeida-Splendore disease<sup>1</sup>.

PCM represents a significant public health challenge, given the susceptibility of young adults in their most productive phase of life (between 30 and 59 years), and the difficult-to-treat nature of the infection<sup>2</sup>.

The route of infection is generally through the upper airways, through which Pb conidia are inhaled. These infectious propagules initially settle in the lungs, but the fungus can then spread throughout the body, causing lesions in the internal mucocutaneous and osteoarticular organs<sup>3,4</sup>.

Osteoarticular involvement becomes chronic in about 60% of cases and occurs secondary to systemic involvement<sup>5</sup>. Articular PCM manifestation involves signs of intense inflammation, including functional impairment of the joint. X-ray examinations

demonstrate cartilage destruction, space reduction, and joint effusion<sup>6</sup>.

However, few studies report evidence-based details regarding articular PCM; the understanding of its evolution is currently based on assumptions found in literature. Thus, this study aimed to evaluate the evolution of Pb-induced experimental arthritis of the knee joint in Wistar rats.

After approval was received from the Research Ethics Committee of UNIOESTE (N. 05/2013), the study was performed in the Laboratory of Microbiology at the State University of Western Paraná, in Cascavel/PR. We used 45-60 day-old Wistar rats (n = 24) randomly and allocated them evenly to either an absolute control group (ACG, which remained uninfected) or 15-day, 45-day, or 90-day experimental groups (which were inoculated with Pb). The animals in the experimental groups were sacrificed after their respective experimental periods had elapsed, and ACG animals were sacrificed at the 90-day mark.

Induction of experimental arthritis took place as described by Loth et al.<sup>7</sup>. The animals were anesthetized with ketamine and xylazine, intraperitoneally (50 mg/kg and 10 mg/kg body weight). Each animal received a medial knee region inoculation using a Pb18 strain cell suspension ( $1 \times 10^5$  yeast cells/ml in

**Corresponding author:** Vanessa Cecatto.

**e-mail:** vane\_cecatto@hotmail.com

**Received** 5 February 2018

**Accepted** 21 June 2018

phosphate buffered saline (PBS)). Viability of suspended cells was above 90%, as confirmed by the Trypan Blue assay. ACG animals underwent the same procedure, using only PBS.

To monitor the evolution of edema, laterolateral diameter measurements (mm) of the right knee joint in extension were made periodically using a Western digital caliper. The baseline measurement occurred prior to Pb18 inoculation, and the final measurement was done just prior to sacrifice.

At the end of each experimental group interval, the corresponding animals were anesthetized using intraperitoneal ketamine and xylazine (50 mg / kg, 20 mg / kg body weight) and sacrificed through the guillotine. Blood was collected for immunological analysis, including ELISA-based assessment of anti-gp43 antibody titers as described by Ramos et al.<sup>8</sup>

For histological analysis, the right knee joint of each animal was dissected and fixed in 10% formalin buffered solution, followed by a routine protocol to embed the tissue in Paraffin. Longitudinal microsections of 7  $\mu$ m thickness were stained with hematoxylin and eosin for morphological analysis, and with Grocott's stain to evaluate Pb18 infection, prior to examination using light microscopy.

Differences between groups of ELISA absorbance readings were statistically compared using an ANOVA. Edema measurements were statistically compared using the Wilcoxon test. Both comparisons were performed using *GraphPad Prism*®, version 3.0 for *Windows XP*, *Microsoft Office*®, and results were considered statistically different at a 5% significance level.

Joint edema increased in the Pb18-infected group, peaking on day 15, followed by a decrease up to day 45, and then a plateau until day 90. The increase in joint edema varied between 30% and 40% of baseline thickness (**Figure 1**).

Titers of anti-gp43 antibodies against Pb exhibited a progressive increase until day 45, after which the level at day 90 was reduced, but still higher than that observed at day 15 (**Figure 2**).

Qualitative histological analysis demonstrated that Pb18-mediated synovitis was established by day 15, including granulomatous inflammation exhibiting poorly organized granulomas and edema in the perimeniscal region synovial membrane, inflammatory cells in the intima and sub-intima, and increased intimal thickness as well as neovascularization. **Figure 3A** shows the part of the ACG joint, with anatomical aspects preserved for comparison. Morphology of other articular tissues (cartilage of the femur and tibia), as well as of the subchondral bone was normal (**Figure 3B**).

At 45 days post-infection, the experimental group exhibited exacerbation of pathology, including pannus formation. Synovial membrane inflammatory infiltrates became larger, more intense, and more diffuse, affecting its full thickness and with the presence of marked neovascularization. Numerous, dense Pb18-containing granulomas were observed, whereas Langhan's giant cells and empty Pb18 capsules were less frequently observed (**Figures 3C** and **3D**).

At 90 days post-infection, large granulomas had formed in the synovial membrane (**Figure 3E**), with Pb18 localizing to joint-adjacent regions, including the perimuscular region, with

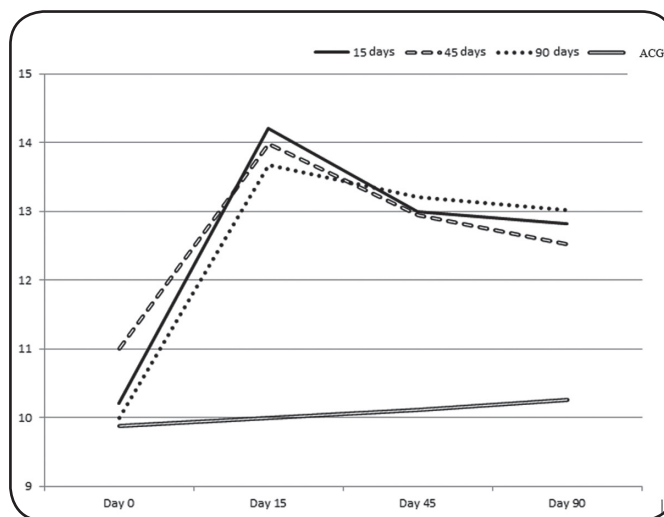


**FIGURE 1:** Joint edema dynamics throughout the experimental interval. Multiple comparisons performed using an ANOVA (Tukey *post-hoc*) demonstrated the presence of a statistically significant difference in experimental group edema between the beginning and end of the experimental interval ( $p=0.0001$  15-day Group,  $p=0.005$  45-day Group, and  $p=0.005$  90-day Group).

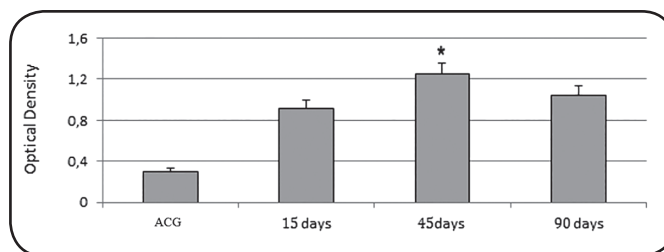


**FIGURE 2:** Titers of anti-gp43 antibodies against Pb. Peak antibody titers were observed at 45 days. Multiple comparisons performed using an ANOVA (Tukey *post-hoc*) demonstrated a statistically significant difference between the day 45 group and the other groups. (\* $p = 0.002$ ).

areas of lytic necrosis (**Figure 3F**). The main pathological finding at this timepoint was the presence of Pb18 in the subchondral bone of the femur and tibia (**Figure 3G** and **3H**).

Edema formation peaked at day 15, had somewhat abated by day 45, and had stabilized by day 90. These results agree with the findings of a similar study, in which a considerable increase in edema was also observed in the experimental groups at days 15 and 45 post-induction of infection<sup>9</sup>.

The day 45 experimental group exhibited an increase in titers of anti-gp43 antibody against Pb18, indicating persistence and progression of the disease. However, at day 90, a reduction in antibody titers was observed. This agrees with the findings of a similar study, in which researchers monitored anti-gp43 expression at days 15 and 45 in the same experimental model, and observed an increase in titers at day 45, possibly due to fungal proliferation<sup>10</sup>.

In this study, although dissemination and spread of the disease had occurred by day 90 as demonstrated by the

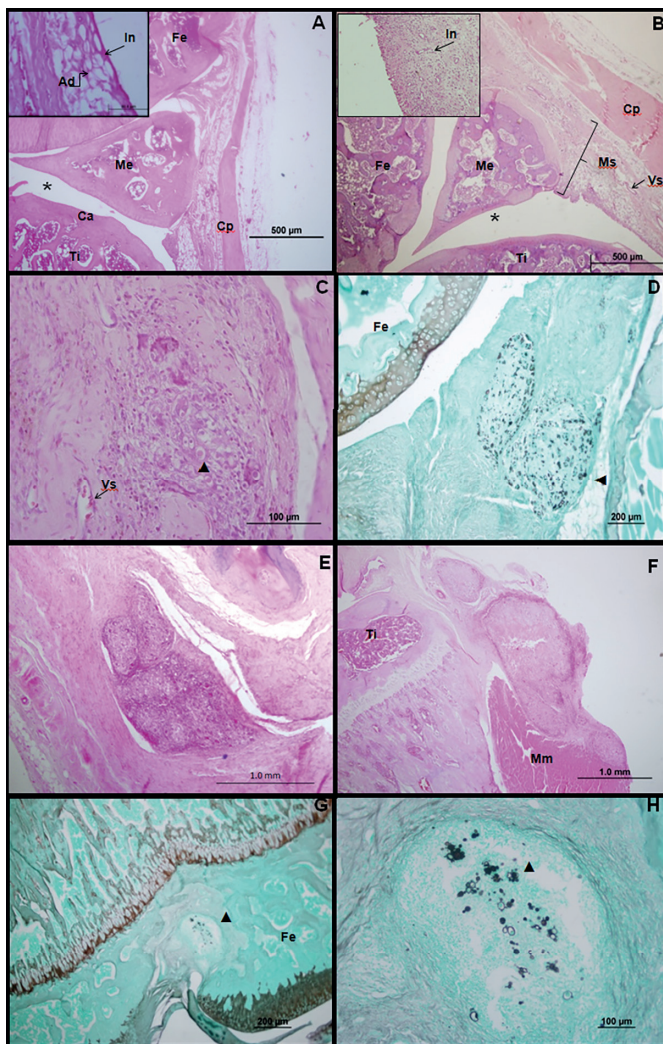


**FIGURE 3:** Wistar rat knee joint sagittal section photomicrographs. Sections A, B, C, E, and F were stained with Hematoxylin and Eosin; sections D, G, and H were stained using the Grocott's stain. **A:** control group with preserved anatomical aspects: articular cartilage (Ca), cavity (\*), meniscus (Me), joint capsule (Cp), femur (Fe), and tibia (Ti). Inset shows details of the synovial membrane, including synoviocytes (arrow) and sub-intima exhibiting a predominance of adipose (Ad) cells. **B:** Day 15 experimental group: synovitis with granulomatous inflammation and edema at the synovial membrane (Ms) of the perimeniscal region, as well as sub-intimal neovascolarization (Vs). Inset shows details of the intimal layer (In), which exhibited thickening. **C and D:** Day 45 experimental group: synovial membrane with pannus containing granulomas featuring fungi (tip of the arrow). **E to H:** Day 90 experimental group. **E:** Synovial membrane exhibiting mature granulomas (delimited by a dashed line). **F:** Mature granulomas (delimited by a dashed line) located in joint-adjacent regions and perimuscularly (Mm), with areas of lytic necrosis. **G and H:** Presence of Pb (tip of the arrow) in the subchondral bone of the femur.

anatomical pathology examination, the animals' immune systems failed to maintain antibody titers. This agrees with the findings of a study in which patient plasma levels of anti gp-43 antibody exhibited a significant elevation on day 28 post-infection, but a reduction on day 56 post-infection, even in the absence of treatment<sup>11</sup>.

During the evaluation of anatomical pathology, classical signs of PCM were observed in the experimental groups. At day

15 post-infection, synovitis with granulomatous inflammation, edema, an inflammatory infiltrate, and neovascolarization predominated. This agrees with human case reports in which the presence of numerous Pb elements of varying sizes (including multiple budding elements) and the presence of fungus-containing Langhan's giant cells amidst macrophages was observed<sup>12</sup>.

In this study, infection severity was higher on day 45 compared to day 15, as evidenced by pannus formation, increased synovial membrane edema, severe synovitis, severe neovascolarization, periosteal granuloma, necrosis, and periarticular dissemination. Similarly, a clinical study using magnetic resonance imaging also found soft tissue reactive edema and synovial inflammation in PCM patients with joint involvement<sup>13</sup>.

During prior development of the experimental model employed in this study, intense inflammatory signs and focal necrosis occurred at day 45 of exposure<sup>7</sup>. In the current study, lytic necrosis was only observed to be present by day 90. This may be due to virulence of the fungal strain used for inoculation; although both studies used the Pb18 strain, inoculum virulence was not verified in either study. Clinical studies, too, report the presence of well-defined osteolytic lesions in patients<sup>14</sup>.

In the current study, the presence of Pb18 was observed in joint-proximal regions, including perimuscularly, by day 90 post-infection.

Similarly, by day 90 post-infection, Pb appeared in the subchondral bone of the femur and tibia (figures 3G and 3H), underlying the entry point of the middle genicular artery. This suggests that dissemination of the fungus to this location occurred via this vessel. In a retrospective study examining seven clinical cases of osteoarticular PCM, involvement of the bony tissue was observed in all patients, with over 40% of samples exhibiting multiple bone lesions<sup>14</sup>.

The current study pioneers investigation into the evolution and later stages of experimental Pb-induced arthritis, and an attempt has been made to contextualize findings despite the paucity of prior literature. The experimental model of Pb-induced arthritis employed by this study performed satisfactorily for the purpose of studying arthritis evolution.

Based on these results, it would appear – at least in a rodent model - that untreated PCM progresses over time, including development of characteristic anatomical pathology findings such as necrosis and dissemination to adjacent tissues. Despite disease progression, however, a decrease in titers of anti-gp43 antibodies against Pb can be expected.

**Acknowledgements:** Center of Physical Rehabilitation of UNIOESTE.

**Conflict of Interest:** The authors declare that there is no conflict of interest.

## REFERENCES

1. Lacaz CS. Tratado de micologia médica. 9a ed. São Paulo: Sarvier, 2002.
2. Negroni R. Paracoccidioidomycosis (South American blastomycosis, Lutz's mycosis). *Int J Dermatol.* 1993;32(12):847-59.

3. Franco M, Montenegro MR, Mendes RP, Marques SA, Dillon NL, Mota NGS. Paracoccidioidomycosis: a recently proposed classification of its clinical forms. *Rev Soc Bras Med Trop.* 1987;20(2):129-32.
4. Shikanai-Yasuda MA, Telles Filho FQ, Mendes RP, Colombo AL, Moretti ML. Consenso em paracoccidioidomicose. *Rev Soc Bras Med Trop.* 2006;39(3):297-310.
5. David A, Telöken MA, Dalmina V, Oliveira GK, Oliveira RK. Paracoccidioidomicose óssea: relato de caso. *Rev Bras Ortop.* 1997;32(3):254-6.
6. Baransky MC, Silva AF, Rodrigues D. Lesões ósseas e osteoarticulares. In: Del Negro G, Lacaz CS, Fiorillo AM, editores. *Paracoccidioidomicose: blastomicose sul-americana.* São Paulo: Sarvier-Edusp; 1982. p.211-9.
7. Loth EA, Biazim SK, Paula CR, Simão RCG, Franco MF, Puccia R, et al. Experimental Model of arthritis induced by *Paracoccidioides brasiliensis* in rats. *Mycopathologia* 2012;174(3):187-91.
8. Ramos SP, Sano A, Ono MA, Camargo ZP, Estevão D, Miyaji M, et al. Antigenuria and antigenaemia in experimental murine paracoccidioidomycosis. *Med Mycol.* 2005;43(7):631-6.
9. Biazim SK, Loth EA, Ferreira JRL, Antunes J, Silva JR, Gandra RF. Avaliação radiológica e do edema no modelo Experimental de artrite fúngica por *Paracoccidioides brasiliensis*. [Apresentação no V Congresso Paranaense de Fisioterapia; 2011 Set-Out 29-03; Paraná, Brasil].
10. Loth EA, Biazim SK, Santos JHFF, Puccia R, Brancalhão RC, Chasco LF, et al. Dose Response Effect Of *Paracoccidioides Brasiliensis* In An Experimental Model Of Arthritis. *Rev. Inst. Med. trop. S. Paulo* 2014;56(3):259-64.
11. Tatibana BT, Sano A, Uno J, Mikami Y, Miyaji M, Nishimura K, et al. Resposta imune humoral na paracoccidioidomicose experimental em camundongos. *Semin: Ciênc. Agrár.* 2007;28(2):287-94.
12. Silvestre MTA, Ferreira MS, Borges AS, Rocha A, Souza GM, Nishioka SA. Monoartrite de joelho como manifestação isolada de paracoccidioidomicose. *Rev. Soc. Bras. Med. Trop.* 1997;30(5):393-95.
13. Savarese LG, Monsignore LM, Andrade-Hernandes M, Martinez R, Nogueira-Barbosa MH. Magnetic resonance imaging findings of paracoccidioidomycosis in the musculoskeletal system. *Trop. Med. Int. Health.* 2015;20(10):1346-54.
14. Lima Junior FVA, Savarese LG, Monsignore LM, Martinez R, Nogueira-Barbosa MH. Aspecto de imagem da Paracoccidioidomicose osteoarticular na avaliação por tomografia computadorizada. *Radiol Bras.* 2015;48(1):1-6.